Spectral hole burning effects initiated by uniform signal intensities in a gain-flattened EDFA

A. R. Sarmani[1], S-J Sheih[2], F. R. Mahamd Adikan[3], and M. A. Mahdi[1*]

[1] *Wireless and Photonics Networks Research Center, Faculty of Engineering, Universiti Putra Malaysia, Selangor 43400, Malaysia*

[2] *Taiwan International Securities Group, Taipei 106, China*

[3] *Department of Electrical Engineering, Faculty of Engineering, Universitiy of Malaya, Kuala Lumpur 50603, Malaysia*

[*] *Corresponding author: mdadzir@eng.upm.edu.my*

Received July 25, 2010; accepted October 21, 2010; posted online January 28, 2011

Spectral hole burning (SHB) effects in a gain-flattened erbium-doped fiber amplifier (EDFA) are demonstrated to be significant in the presence of large signal power around the 1530−1532-nm wavelength range. These are the first effects reported in a setup employing equivalent power level distribution of 40 channels ranging from 1530 to 1561 nm. To explain this, the introduction of a new local population variable into the laser equation is required to support the original inversion ratio that is determined by the pump lasers. In the analysis section, spectroscopic parameters and high signal powers are considered to be other contributing parameters to the change in the gain characteristics. An improvement to this theoretical basis is suggested by implementing mathematical modeling to validate similarities between the gain shape of simulation to that obtained in the experiment.

OCIS codes: 060.2320, 060.2410, 060.0060.

doi: 10.3788/COL201109.020603.

The increasing demand for extensive bandwidth data transmission rate in optical fiber communications has elevated scientific and industrial efforts to develop high-capacity wavelength division multiplexing (WDM) systems. This can be realized by exploiting the broad bandwidth property of an erbium-doped fiber amplifier (EDFA) that can cover the lowest attenuation telecommunication window of around 1.5 μm. However, the performance of WDM relies strictly on the gain property of the EDFA. In designing WDM devices for long-haul communications, maintaining the gain uniformity of the amplifier can be difficult.

To resolve this, optical filters have been developed to ensure consistency in the gain operation[1−3]. It has been demonstrated previously that in the C-band of EDFA that covers 32-nm bandwidth, the wavelength-independent gain spectra are generated within a tolerance of around ± 0.75 dB[4]. These are characterized when a gain equalization filter (GEF) is employed in the intracavity arrangement. However, variations in the gain shape can still occur even though the original gain feature is earlier designed to be perfectly leveled. This is caused by the occurrence of spectral hole burning (SHB), owing to the existence of strong optical powers. This degrades the amplifier performance with the onset of unnecessary nonlinear effects.

SHB demonstrates more impacts at the shorter wavelength range of around 1530 nm compared with that in the extended wavelengths[5,6]. In previous research, it was reported that a hole depth as small as 0.1 dB was produced for a 4-dB gain compression in the 1545−1560-nm wavelength domain[7]. Some researchers have also found that the spectral hole depth and width were functions of saturating signal wavelength and power[5,7−9]. It was also previously discovered that the shape of the spectral hole was complex and thus cannot be characterized by a simple Gaussian distribution[10]. As a result, several advancements to the previous models have been suggested to further elaborate the physical background of SHB[11−13].

The laser gain in an EDFA is typically determined by the population inversion ratio, which depends on the pump wavelength[14]. However, this is not necessarily accurate due to the correlations between the incoming powers and the spectroscopic properties to the spectral profiles at the corresponding signal wavelengths. Thus, an additional local deviation must be introduced into the gain equation. To the best of our knowledge, the impact of uniform signal powers across the gain-flattening bandwidth has never been studied yet. Therefore, in this letter, we investigate the SHB effects induced by identical power distribution of WDM signals in the four-stage EDFA. The results obtained are analyzed and mathematical explanations are suggested to further understand the underlying physics behind this SHB phenomenon.

The experimental layout of the gain-flattened EDFA (GF-EDFA) is illustrated in Fig. 1(a), wherein the EDF has a gain bandwidth of 35 nm for the wavelength range of between 1529 to 1564 nm. This layout comprised four amplifier stages (EDFA #1, #2, #3, and #4) that included three embedded optical devices between the amplifier elements, as previously reported in Ref. [15]. These optical devices included a dispersion compensating module (DCM), a variable optical attenuator (VOA), and a GEF.

The DCM was utilized to offset the nonlinear effects in the dispersive fiber that could affect the signal quality performance. It introduced a maximum loss of 10 dB, which was important for the attainment of wavelength-independent gain spectra from the amplifier. Meanwhile,

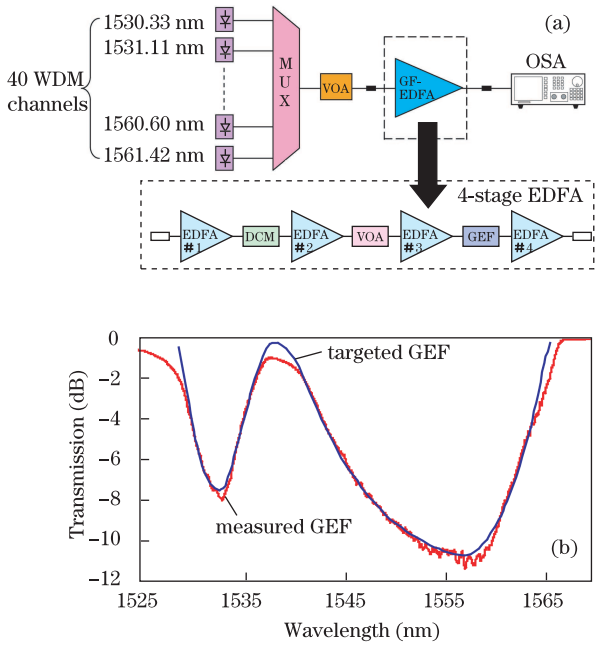

Fig. 1. (a) Experimental setup to study the effect of SHB in a GF-EDFA, with the amplifier inside the rectangular box being composed of four-stage EDFA and (b) spectral transmission of the measured and targeted GEFs.

a VOA was employed to adjust the gain operating value from 15 to 30 dB. In addition, the GEF was incorporated to maintain an equal gain level within a variation of around ± 0.75 dB. The spectral transmission of this filter, as demonstrated in Fig. 1(b), is designed to satisfy the inversion population ratio at 977 nm. From the figure, higher losses are introduced in the wavelength band where the gain is higher. The two minimum valleys observed in this spectral curve represent the maximum losses of 8 and 11 dB around 1530 and 1557 nm, respectively. As shown in Fig. 1(b), the targeted GEF curve was obtained from the design phase in which the four-stage EDFA exhibited a flat gain over the intended wavelength range. The targeted GEF curve was set as the reference data, and the GEF error function was obtained by comparing these two GEF curves. The error function was then utilized as the benchmark to evaluate the impact of SHB on WDM signals.

The pump sources for EDFA #1, #2, and #3 were provided at 977 nm. However, the remaining EDFA #4 was pumped by two lasers at 1480 nm to reach an output power level of up to 23 dBm. The latter pump wavelength (1480 nm) was included to support better power conversion efficiency because of its closer distance to the signal. During the experiment, the pump powers were controlled simultaneously to facilitate the gain-flattening operation. The input of 40 WDM channels was connected by a multiplexer (MUX) with a 100-GHz spacing. The total input power was adjusted by another VOA just before the GF-EDFA. In such case, the measurement of gain was completed by using an optical spectrum analyzer (OSA).

At the outset of this research, the input signal powers (40 channels) were determined in a dynamic range from −26 to −11 dBm (small signal powers). A series of corresponding gain from 30 to 15 dB was produced by tuning the VOA from 0 to 15 dB. The pump lasers were also controlled simultaneously in order to manage the total output power at a constant 4 dBm. In the entire assessment, 977-nm pump sources were maintained for EDFA #1, #2, and #3 to confirm that the population inversion ratio was fixed at $\bar{n}_2$. Uniform gain spectra from the amplifier were expected to be in agreement with the theoretical elaboration that was given in Refs. [14] and [16].

Figure 2 depicts the normalized gain that is deduced based on the difference between the measured and targeted gain values for various signal powers. The GEF error function is also plotted as the benchmark for the evaluation of similar gain levels. In general, the trend of gain pattern is in good agreement with the error function, wherein the output shape that complies to this feature resulted in a straight line. This is confirmed for the wavelengths that are longer than 1532 nm, where the supposedly equal gain level is generated, as shown in Fig. 2. In contrast, the gain curve that deviates from the error function shows a small increase. A slight gain distortion of around 0.6 dB is observed for wavelengths that are less than 1532 nm. The error has similar pattern to that produced at longer wavelengths where its value is almost similar for each input power level. This is mainly contributed by the discrepancy in spectral-dependent losses of the GEF transmission profile during the design stage compared with that during the implementation.

To further study this physical issue at different wavelengths, another experiment was carried out at higher powers. The input signal powers were modified from −7 to 8 dBm for the gain of 30 to 15 dB, respectively. The pump lasers were then adjusted to stabilize the output power at 23 dBm, and the results obtained are presented in Fig. 3. In a full analogy to the graph shown in Fig. 2, a gain increment is observed again at a shorter wavelength region ($\lambda_s \leq 1532$ nm). However, the increasing values are more significant and different with respect to the signal powers.

This effect is assumed to occur because of SHB[11,17]. Thus further analysis is required to explain this phenomenon through the introduction of new variable $\bar{n}_2^{(i)}$[17], instead of $\bar{n}_2$[14], into the laser gain. Based on the homogenous model, $\bar{n}_2^{(i)}$ denotes the average fractional population at the metastable level. With its inclusion, the laser gain at the signal wavelength $G(\lambda_s)$[17] can be

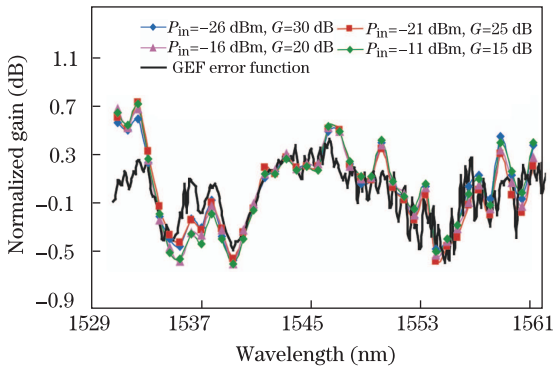

Fig. 2. Normalized gain spectra in comparison with the GEF error function; the combined output power is 4 dBm, in which the input signal powers alter from −26 to −11 dBm.

transformed into the following

$$G(\lambda_s) = \sum_{pop.i} \left[\bar{n}_2^{(i)} (g_i^* + \alpha_i) - \alpha_i \right], \quad (1)$$

where $\bar{n}_2^{(i)} = \overline{N}_2^{(i)} / N_{tot}^{(i)}$ comprises the ratio between the average population density at the excited level $\overline{N}_2^{(i)}$ and the total populations at both ground and upper states $N_{tot}^{(i)}$. *pop.i* refers to the total population at both ground and upper states where the value may change from one sub-population to another, Therefore, the superscript i on these parameters demonstrates variations within the sub-population to another. Other spectroscopic properties that include g_i^* and α_i are the emission and absorption coefficients, respectively. These are as described as

$$g_i^* = 10 \lg(e) \Gamma(\lambda_s) N_{tot}^{(i)} \sigma_e^{(i)}(\lambda_s) \quad (2a)$$

and

$$\alpha_i = 10 \lg(e) \Gamma(\lambda_s) N_{tot}^{(i)} \sigma_a^{(i)}(\lambda_s), \quad (2b)$$

where $\Gamma(\lambda_s)$ is the overlap factor between the optical mode intensity and the erbium doping distribution and the cross-sections of $\sigma_e^{(i)}$ and $\sigma_a^{(i)}$ signify those for emission and absorption, respectively.

However, by involving the SHB effect in the output gain spectrum that leads to the gain distortions, a few characteristics can be introduced into $\bar{n}_2^{(i)}$. This inversion ratio at population i[14,15] can then be expressed as

$$\bar{n}_2^{(i)} = n_{ave}(\lambda_p, z) + \Delta n_{SHB}(\lambda_s, z), \quad (3)$$

where $n_{ave}(\lambda_p, z)$ is the average population inversion ratio at position z that is influenced by the pump wavelength λ_p and $\Delta n_{SHB}(\lambda_s, z)$ is the inversion ratio induced by the SHB effect. The latter factor implies dependency on the signal wavelength λ_s as well as the position z. For signal wavelengths that are longer than 1532 nm, $\Delta n_{SHB}(\lambda_s, z)$ is 0, thus Eq. (3) becomes $\bar{n}_2^{(i)} = n_{ave}(\lambda_p, z)$. The utilization of 977-nm pump sources in the entire evaluation ensures that the population inversion ratio at population z is maintained at $n_{ave}(\lambda_p, z)$ with the absence of SHB effect, as reported previously in Ref. [4]. However, for wavelengths shorter than 1532 nm, $\Delta n_{SHB}(\lambda_s, z)$ has a finite value, where $\bar{n}_2^{(i)}$ is composed of both factors as manifested in Eq. (3).

From this theoretical elaboration, it is concluded that the gain dynamic changes $\Delta G(\lambda_s)$ shown in Fig. 3 at shorter λ_s are initiated by $\Delta n_{SHB}(\lambda_s, z)$, which is inclusive in Eq. (1). On the other hand, the adherence of the gain line to that of GEF error function implied a flat gain spectrum at a longer wavelength range ($\lambda_s \geq 1532$ nm). These can be clarified from the role of spectroscopic factors that are constituted in Eqs. (1) and (2), where $G(\lambda_s) \propto \bar{n}_2^{(i)} \left[\sigma_e^{(i)} + \sigma_a^{(i)} \right] - \sigma_a^{(i)}$. The maximum summation of $\left[\sigma_e^{(i)} + \sigma_a^{(i)} \right]$ at shorter wavelengths induced significant SHB effects in the gain spectra are compared with those at longer wavelengths, as shown in Fig. 3.

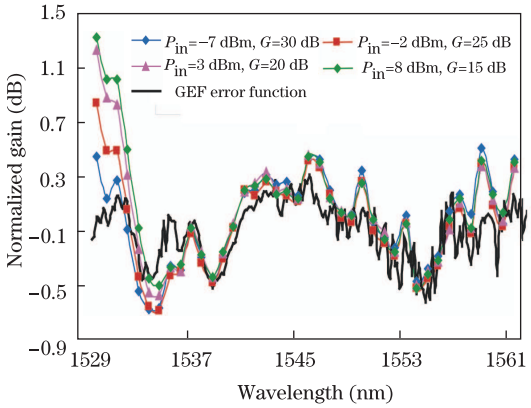

Fig. 3. Correlation between the GEF error function and the spectral pattern of the normalized gain; the output power is maintained at 23 dBm for the corresponding signal powers that were varied from −7 to 8 dBm.

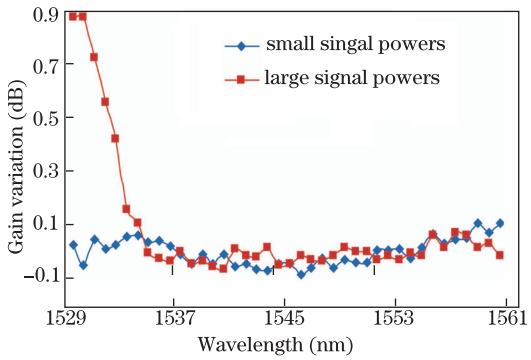

Fig. 4. Comparison of the gain variation between the small signal powers from Fig. 2 and the high signal powers from Fig. 3; gain dynamics are obtained at large signal powers for $\lambda_s < 1534$ nm.

In the analysis, outcomes of the two previous experiments are investigated in details. At the specified signal wavelength λ_s, the differences between the maximum and the minimum values for small and high signal powers are deduced separately from Figs. 2 and 3. These are then compared together and plotted in Fig. 4, where the gain fluctuation at small powers can be taken as the main reference. No experiment was conducted for the intermediate power level because we want to study the importance of SHB at high powers (see Fig. 3). Alternatively, the orientation of gain modulation at other power levels can be estimated from the spectral feature presented in Fig. 4. In this case, the small signal powers produce limited impact on the output spectrum within a tolerance of 0.15 dB in the C-band.

The same finding is observed at large signal powers when the signal wavelength is longer than 1535 nm. On the other hand, at λ_s of around 1530 nm, a maximum gain variation of up to 0.87 dB is measured. These indicate that the gain dynamics is strongly influenced by the intensity of the optical powers where the SHB effect is proportional to the elevation in signal powers, as shown in Fig. 3. This mechanism can be explained during lasing, wherein more inverted populations at the excited state decayed radiatively to the ground state along with the increase of the incoming signal powers. As more gen-

eration of photons are initiated, the number of emission cross-section $\sigma_{\rm e}^{(i)}$ is amplified. As $G(\lambda_{\rm s}) \propto \sigma_{\rm e}^{(i)}$, this leads to the expansion of the output gain. It can also be predicted from these evaluations that the development of gain variation at moderate signal powers is in between that of the small and high powers at shorter wavelengths ($\lambda_{\rm s} \leq 1535$ nm). However, equal gain shapes are induced at all power levels at longer wavelengths. Further enhancement to these assessments is suggested by implementing a mathematical modeling to compare the simulation results of the SHB heights to those acquired experimentally[12,13].

In this research, we have observed the existence of SHB effect in the gain output of EDFA with the inclusion of a GEF. This physical scheme is manifested by the substantial spectral height at wavelengths shorter than 1532 nm, which corresponds to the largest summation of cross-section properties, $(\sigma_{\rm e}^{(i)} + \sigma_{\rm a}^{(i)})$. Theoretical derivation of this phenomenon is accomplished by introducing a new variable $\bar{n}_2^{(i)}$, instead of $\bar{n}_2$ into the laser gain equation $G(\lambda_s)$. $\bar{n}_2^{(i)}$ comprises $n_{\rm ave}(\lambda_{\rm p}, z)$ and $\Delta n_{\rm SHB}(\lambda_{\rm s}, z)$, which are the main criteria that elucidate the gain behavior in the C-band of EDFA. However, at extended wavelengths ($\lambda_{\rm s} \geq 1532$ nm), the gain pattern follows the characteristic of GEF error function, implying a stable gain level operation. When the signal powers increase to higher values, more considerable gain dynamics $\Delta G(\lambda_s)$ are produced at shorter $\lambda_{\rm s}$. This indicates the proportionality between the gain increase to the incoming signal powers due to the greater conversion of inverted populations into photons. This leads to the rise in emission cross-section $\sigma_{\rm e}^{(i)}$, which justifies this output increment. The effect of SHB must be taken into consideration in amplifying multiple channels simultaneously by adding additional loss at the signal wavelengths shorter than 1532 nm.

This work was partly supported by the Ministry of Higher Education, Malaysia, and the Universiti Putra Malaysia under the post-doctoral research fellowship scheme.

References

1. P. F. Wysocki, J. Judkins, R. Espindola, M. Andrejco, A. Vengsarkar, and K. Walker, IEEE Photon. Technol. Lett. **9,** 1343 (1997).
2. M. Harurnoto, M. Shigehara, and H. Suganuma, J. Lightwave Technol. **20,** 1027 (2002).
3. R. K. Vashney, B. Nagaraju, A. Singh, B. P. Pal, and A. K. Kar, Opt. Express **15,** 13519 (2007).
4. A. R. Sarmani, M. A. Mahdi, S. J. Sheikh, and F. R M. Adikan, Laser Phys. **20,** 1-5 (2010).
5. J. W. Sulhoff, A. K. Srivastava, C. Wolf, Y. Sun, and J. L. Zyskind, IEEE Photon. Technol. Lett. **9,** 1578 (1997).
6. S. Jarabo, I. J. Sola, and J. S. Landete, J. Opt. Soc. Am. B **20,** 1204 (2003).
7. A. K. Srivastava, J. L. Zyskind, J. W. Sulhoff, J. D. Evankow, Jr., and M. A. Mills, in *Proceedings of Optical Fiber Communication Conference 1996* TuG7 (1996).
8. I. Joindot and F. Dupre, Electron. Lett. **33,** 1239 (1997).
9. S. Ono, S. Tanabe, M. Nishihara, and E. Ishikawa, J. Opt. Soc. Am. B **22,** 1594 (2005).
10. E. Rudkevich, D. M. Baney, J. Stimple, D. Derickson, and G. Wang, IEEE Photon. Technol. Lett. **11,** 542 (1999).
11. M. Bolshtyansky, J. Lightwave Technol. **21,** 1032 (2003).
12. M. Nishihara, Y. Sugaya, and E. Ishikawa, in *Proceedings of Optical Amplifiers and Their Applications 2003* TuD3 (2003).
13. M. Nishihara, Y. Sugaya, and E. Ishikawa, in *Proceedings of Optical Fiber Communication Conference 2004* FB1 (2004).
14. M. J. Yadlowsky, IEEE Photon. Technol. Lett. **11,** 539 (1999).
15. M. A. Mahdi, S. J. Sheih, and F. R M. Adikan, Opt. Express **17,** 10069 (2009).
16. C. R. Giles and E. Desurvire, J. Lightwave Technol. **9,** 271 (1991).
17. M. J. Yadlowsky, J. Lightwave Technol. **17,** 1643 (1999).